

Nonequilibrium electron spectroscopy of Luttinger liquids

So Takei, Mirco Millettari, and Bernd Rosenow

Max-Planck-Institut für Festkörperforschung, D-70569 Stuttgart, Germany

(Dated: February 22, 2024)

Understanding the effects of nonequilibrium on strongly interacting quantum systems is a challenging problem in condensed matter physics. In dimensions greater than one, interacting electrons can often be understood within Fermi-liquid theory where low-energy excitations are weakly interacting quasiparticles. On the contrary, electrons in one dimension are known to form a strongly-correlated phase of matter called a Luttinger liquid (LL), whose low-energy excitations are collective density waves, or plasmons, of the electron gas. Here we show that spectroscopy of locally injected high-energy electrons can be used to probe energy relaxation in the presence of such strong correlations. For detection energies near the injection energy, the electron distribution is described by a power law whose exponent depends in a continuous way on the Luttinger parameter, and energy relaxation can be attributed to plasmon emission. For a chiral LL as realized at the edge of a fractional quantum Hall state, the distribution function grows linearly with the distance to the injection energy, independent of filling fraction.

Over the last decade, experimental advances in nanostructure fabrication have brought a resurgence of interest in the LL model because of the possibility to test its peculiar predictions [1, 2, 3, 4, 5]. Defining signatures of a LL such as spin-charge separation [6, 7], charge fractionalization [8, 9], and the power-law suppression of the local electron tunneling density of states [10, 11, 12, 13, 14] have been experimentally verified. Recently, LLs driven far from equilibrium have begun to receive attention [15, 16, 17, 18]. Studying these systems offers the possibility to characterize novel aspects of electron-electron interactions and to understand energy relaxation processes that have not been apparent in the above-mentioned equilibrium experiments.

Here we consider a LL driven out of equilibrium by local injection of high-energy electrons, far away from any contacts, at a fixed energy. Their spectral properties are extracted at another spatial point some distance away by evaluating the average tunneling current from the LL into an empty resonant level with tunable energy. In this work, we consider both standard (non-chiral) and chiral LLs, which are realized at the edge of fractional quantum Hall systems [3, 4, 12, 13, 14].

For the standard LL and for probe energies slightly below the injection energy, we find that the inelastic component of the current shows a power law behavior as a function of the difference between injection and detection energy, with an exponent that continuously evolves as the interaction parameter is varied. We develop a perturbative approach which shows how injected electrons can relax by emitting plasmons inside the wire.

For a chiral LL at the edge of a fractional quantum Hall state from the Laughlin sequence, an essentially exact calculation of the tunneling current is possible. Here, the inelastic part of the electron current *increases* in a linear fashion as the probe energy is lowered from the injection energy towards the chemical potential of the edge state, despite a *decreasing* tunneling density of states for electrons. This behavior is compatible with our result for the standard LL in the limit of strongly repulsive interactions. For probe energies close to the chemical potential, the chiral LL is far from equilibrium: the electron

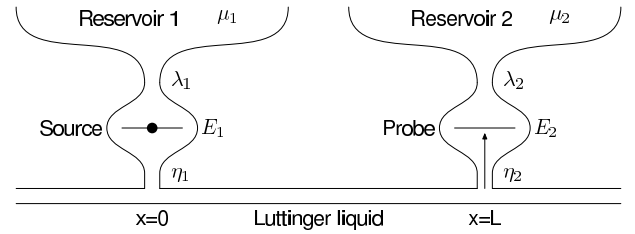


FIG. 1: **The proposed experimental setup.** Hot electrons are injected from the source resonant level at $x = 0$, and are collected at the probe resonant level at $x = L$. System parameters are set (see text) so that the source (probe) occupancy is fixed to be full (empty). Spectral properties of the injected electrons are extracted by measuring the tunneling current between the edge and the probe (indicated by the arrow).

spectral function approaches a finite value, in striking contrast to the power law decrease towards zero in equilibrium. In addition to the inelastic contribution to the probe current, in a chiral LL there always is an elastic contribution, indicating that a finite fraction of electrons travels from the injection to the probe site without losing energy.

Electrons with charge e_0 are injected into the LL from a resonant level (source) with energy $E_1 \equiv e_0 V_1 > 0$ at position $x = 0$ (see Fig.1). Energy relaxation is studied by coupling a second resonant level (probe) with energy $E_2 \equiv e_0 V_2 > 0$ to the LL at position $x = L$ (downstream for the chiral LL), and by computing the tunneling electron current between the LL and that level. The two levels are coupled to the LL via tunneling amplitudes η_1 and η_2 , respectively. In addition, source and probe dots are coupled to reservoirs held at chemical potentials μ_1 and μ_2 via tunneling amplitudes λ_1 and λ_2 . The chemical potential of the LL is taken to be zero. We assume the level broadening due to tunnel couplings to be small in comparison to both E_1 and E_2 , and therefore consider the current in the sequential-tunneling regime. Further, we assume $\lambda_1 \gg \eta_1$ with $\mu_1 > E_1$ so that the source occupancy is constrained to one, and $\lambda_2 \gg \eta_2$ with $\mu_2 < E_2$ so that the probe

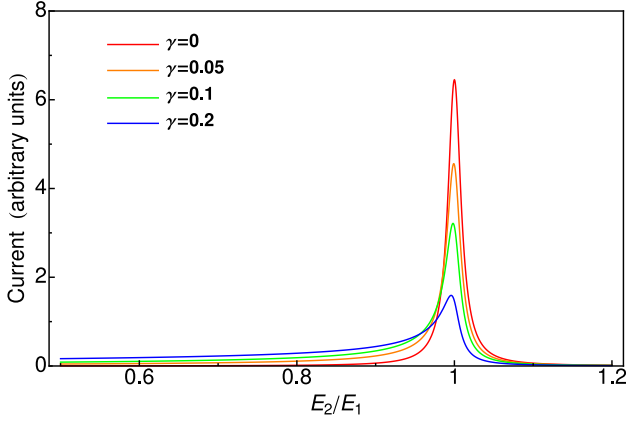


FIG. 2: **Tunneling current for the standard case for various interaction.** The current is plotted for zero temperature and includes the leading contribution in $\Delta E/E_1$. The inelastic contribution for $E_2 < E_1$ shows a power law decay as a function of increasing ΔE with an exponent that depends on the interaction parameter (see text). A level broadening of $0.01E_1$ is used for the elastic peak.

occupancy is fixed at zero.

We first focus on the standard LL and consider spinless electrons, for which the interaction strength is described by a single parameter K [2]. The case $K = 1$ describes non-interacting electrons, $K < 1$ corresponds to repulsive interactions, and $K > 1$ to attractive ones. We use the non-equilibrium Keldysh formalism [19] to calculate the current flowing into the probe dot to leading order in the tunneling amplitudes η_1 and η_2 , details are described in the appendix.

$$I = -\frac{2\pi e_0}{\hbar} \frac{|\eta_1|^2 |\eta_2|^2 \theta(\Delta E)}{u^2 \hbar^2 E_1 \Gamma^2(1 + \gamma)} \left(\frac{\alpha E_1}{u \hbar} \right)^{4\gamma} \left[\frac{(\Delta E/E_1)^{2\gamma-1}}{\Gamma(2\gamma)} \right]. \quad (1)$$

Here, $\Gamma(x)$ is the gamma-function, u is the velocity of plasmon excitations, α denotes the short distance cutoff of the theory, and $\gamma = K(1/K - 1)^2/4 \geq 0$. When calculating the current Eq. (1), the limit of large interdot separation $u/L \ll E_1, E_2$ was taken. In the non-interacting limit ($\gamma \rightarrow 0$) the quantity in the square brackets is a representation of the delta-function, and Eq. (1) reduces to $I \propto \delta(\Delta E)$. When the interactions are turned on, the elastic peak gradually broadens to give rise to an inelastic contribution which shows a power law decay as a function of increasing ΔE , with an exponent that continuously evolves as a function of the interaction parameter. For strong enough interactions with $\gamma > 1/2$, the elastic peak vanishes and the remaining inelastic contribution monotonically increases with a power law which again evolves as a function of the interaction parameter. The result Eq. (1) is plotted in Fig. 2. Broadening of the peak is included in the figure to reflect the finite width of the resonant levels due to the couplings to the reservoirs and the wire.

In the limit of weak interactions with Luttinger parameter K close to one, energy relaxation as described by Eq. (1) can be interpreted by using lowest order perturbation theory in the interaction strength. Interactions can be decomposed into for-

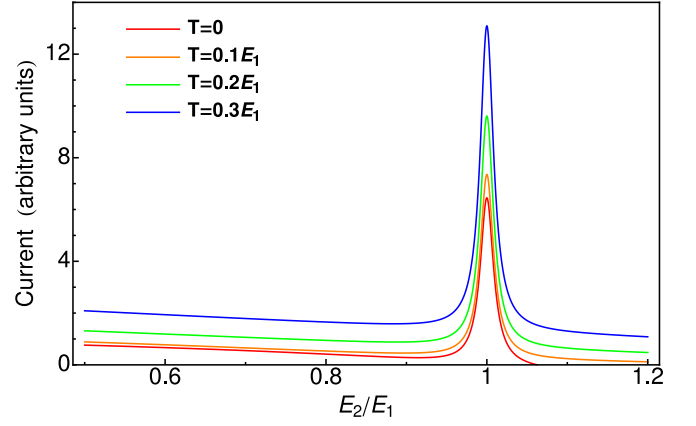


FIG. 3: **Tunneling current for the chiral case at various temperatures.** The current shows an elastic contribution at $E_1 = E_2$, and an inelastic contribution for $E_2 < E_1$ which increases as energy transfer is increased. The broadening of the elastic peak is included as in the standard case. The same level broadening as the standard case is used here.

ward scattering between electrons near the same Fermi point with amplitude g_4 , and between electrons near opposite Fermi points with amplitude g_2 . The g_4 -interaction merely renormalizes the fermion and plasmon velocities and cannot give rise to relaxation. In a spatially homogeneous LL, the g_2 -process cannot give rise to energy relaxation either due to the simultaneous requirement of momentum and energy conservation. However, because of the local nature of injection and collection processes considered here, an electron is capable of exploring virtual momentum states in connection with tunneling, and a consecutive inelastic process can both conserve momentum and produce a final state with the same total energy as the source state. Here, we consider the lowest order inelastic process proportional to $\gamma \propto g_2^2$ at zero temperature, in which an electron is transported from the source to the probe while emitting a single plasmon inside the wire. First, the electron in the source tunnels into a right moving momentum eigenstate whose energy may be different from E_1 . In the second step, a left moving plasmon with energy ΔE is emitted via a g_2 -process, and the right moving electron is scattered into another wire state such that momentum is conserved. After propagation along the wire, the electron tunnels into the probe. Alternatively, tunneling into the wire can be elastic, and the plasmon can be emitted when tunneling into the probe. One finds that the matrix element for these processes scales as $1/\sqrt{|\Delta E|}$. This can be understood by multiplying the matrix element for plasmon emission, which increases as $\sqrt{|\Delta E|}$, with the time available for plasmon emission, which diminishes as $1/|\Delta E|$ due to the energy-time uncertainty principle. The tunnel current can then be computed using Fermi's golden rule, and correctly reproduces the inelastic component $I \propto \gamma/\Delta E$ of equation (1) to order γ .

Next, we consider tunneling into a chiral LL at the edge of a fractional quantum Hall state from the Laughlin sequence. We

focus on the filling fraction $\nu = 1/3$, where the area occupied by one electron is threaded by three quanta of magnetic flux. The calculation of the steady state current proceeds along the

same lines as for Eq. (1), with the difference that we were able to obtain an exact expression for all values of ΔE and for finite temperature,

$$I = -e_0 \frac{\pi^3 |\eta_1|^2 |\eta_2|^2 \alpha^4 (k_B T)^3}{4u^6 \hbar^7} \left[\frac{X_1^2 e^{\frac{X_1}{2}}}{\cosh(X_1/2)} \left(1 + \frac{X_1^2}{\pi^2} \right) \delta(\Delta X) + \frac{3\Delta X e^{\Delta X/2}}{\sinh(\Delta X/2)} \sum_{i=1}^2 \frac{e^{X_i/2}}{\cosh(X_i/2)} \left(1 + \frac{X_i^2}{\pi^2} \right) \right]. \quad (2)$$

Here, $\Delta X = X_1 - X_2$, $X_i = E_i/k_B T$. At zero temperature, the expression for the current simplifies to $I \propto E_1^4 \delta(\Delta E) + 6\theta(\Delta E)(E_1^2 + E_2^2)\Delta E$ where $\Delta E = E_1 - E_2$. The current, plotted for both zero and finite temperatures in Fig.3, has two main contributions: elastic and inelastic. The peak is due to electrons that were elastically transported from the source to the probe. Second, there is a broad inelastic contribution that extends over the range $E_2 < E_1$, and that grows monotonically as E_2 is lowered. For $E_2 \lesssim E_1$, the current increases linearly with ΔE . We have confirmed that a similar inelastic contribution to the current is also present for the Laughlin filling fraction $\nu = 1/5$. In this case, an exact computation at zero temperature shows again that $I_{\text{inel}} \propto \Delta E$ for $E_2 \lesssim E_1$. This suggests that the linear upturn in the current below E_1 may be a generic feature at all Laughlin filling fractions.

For a non-interacting chiral Fermi liquid, which describes the edge excitations of an integer quantum Hall state, hot electrons do not relax. In addition, the weight of the elastic peak is reduced as the temperature is increased. This reduction is due to Pauli blocking of states by thermally excited edge electrons residing above the chemical potential. When interactions are present, Fig.3 shows an overall increase in the elastic current with temperature. This reflects the increase in the tunneling density of states with temperature and constitutes a clear signature of LL physics.

The setup of Fig.1 is ideal for directly extracting the electron energy distribution, $f(E)$, and spectral function, $A(E)$, inside the wire at a spatial point far from the injection site. With the probe occupancy constrained to be empty, the tunneling current is given by $I_{\text{empty}} = ie_0 |\eta_2|^2 G^<(E)$, while a similar evaluation with probe occupation held full gives $I_{\text{full}} = ie_0 |\eta_2|^2 G^>(E)$ [20]. Once the two currents are obtained, both $f(E)$ and $A(E)$ can be extracted by expressing the lesser and greater Green functions, $G^<(E) = if(E)A(E)$ and $G^>(E) = -i(1 - f(E))A(E)$, in terms of electron distribution function and spectral weight. At zero temperature and for $\nu = 1/3$, $f(E_2)$ and $A(E_2)$ valid for $0 < E_2 < E_1$ read

$$A(E_2) = \frac{\alpha^2}{2u^3 \hbar^4} \left[E_2^2 + (E^*)^2 \frac{\Delta E}{E_1} \right], \quad (3)$$

$$f(E_2) = \frac{\left[1 + \left(\frac{E_2}{E_1} \right)^2 \right] \frac{\Delta E}{E_1}}{\left(\frac{E_2}{E^*} \right)^2 + \frac{\Delta E}{E_1}}, \quad (4)$$

where $E^* = \sqrt{6\pi |\eta_1|^2 \alpha^2 E_1^3 / u^3 \hbar^3}$ separates two energy regimes. We note that E^* can be parametrically larger than the level widths such that our sequential tunneling approximation stays valid. In the high-energy regime and for small energy transfers ($E^* \ll E_2 \lesssim E_1$), $f(E_2) \approx 12\pi |\eta_1|^2 \alpha^2 \Delta E / u^3 \hbar^3$, which shows that the linear upturn in the current below E_1 is also reflected in the distribution function. In the same regime, we find that the spectral function does not deviate strongly from its equilibrium expression (with $\eta_1 = 0$). In the low-energy regime ($0 \lesssim E_2 < E^*$), $f(E_2)$ smoothly approaches one and the spectral function approaches a finite value. The latter is in stark contrast to the equilibrium case.

Acknowledgment: We thank A. Yacoby for drawing our attention to the problem of local and energy resolved electron injection, and W. Metzner and V. Venkatachalam for useful discussions. B. R. was supported by the Heisenberg program of DFG.

Appendix: We now provide the theoretical basis for the derivation of Eqs. (1,2). The system is modeled by the Hamiltonian $H = H_{\text{LL}} + H_{\text{dot}} + H_{\text{tun}}$, where H_{LL} models the LL, $H_{\text{dot}} = E_1 \psi_1^\dagger \psi_1 + E_2 \psi_2^\dagger \psi_2$ the two resonant states, and H_{tun} describes the tunneling of electrons between the wire and the two resonant levels. ψ_1 (ψ_2) are electron operators of the source (probe) with occupation numbers $\langle \psi_1^\dagger \psi_1 \rangle = 1$ and $\langle \psi_2^\dagger \psi_2 \rangle = 0$. The standard LL Hamiltonian reads [2]

$$H_{\text{LL}} = \frac{u}{4\pi K} \int dx [(\partial_x \phi_R(x))^2 + (\partial_x \phi_L(x))^2]. \quad (5)$$

where K is the LL parameter, and the left and right moving boson operators satisfy $[\phi_R(x), \phi_R(x')] = -[\phi_L(x), \phi_L(x')] = i\pi K \text{sgn}(x - x')$. One-dimensional electron densities are given by $\rho_{R,L}(x) = (\partial_x \phi_{R,L}(x))/2\pi$ and u denotes the plasmon velocity. To simplify the notation, we use the units where $\hbar = 1$ and $k_B = 1$. The tunneling Hamiltonian is given by

$$H_{\text{tun}} = \eta_1 \psi_1 \psi^\dagger(x=0) + \eta_2 \psi_2 \psi^\dagger(x=L) + h.c. \quad (6)$$

where $\psi(x) = \psi_R(x) + \psi_L(x)$. The electron operators can be bosonized as $\psi_{R,L}(x) = \exp[i(K_\pm \phi_R(x) + K_\mp \phi_L(x))]/\sqrt{2\pi\alpha}$ with $K_\pm = (K^{-1} \pm 1)/2$. The expectation value of the current reads

$$I = \langle T_c \{ \hat{I}_{\text{cl}}(t_1) e^{-i \int_c dt H_{\text{tun}}(t)} \} \rangle_0, \quad (7)$$

where all operators are written in the interaction picture with respect to $H_{LL} + H_{dot}$. The current is computed using the nonequilibrium Keldysh technique [19], and T_c indicates time-ordering of the operators on the time-loop contour c . The “classical” component of the current operator is the symmetric combination of the operator on the forward (+) and backward

(−) parts of the Keldysh contour, i.e. $\hat{I}_{cl}(t) = (\hat{I}_+(t) + \hat{I}_-(t))/2$, where $\hat{I}_\pm(t) = -ie_0[H_\pm, \psi_{2,\pm}^\dagger \psi_{2,\pm}]$. Upon imposing the constraints on the resonant level occupancies and taking the limit of large inter-dot separation, the time of propagation L/u drops out and we arrive at the following expression for the steady state current to leading order in η_1 and η_2 ,

$$I = e_0 |\eta_1|^2 |\eta_2|^2 \int d^3 t e^{-iE_2 t_2 + iE_1 t_3} (iG_{2\gamma+1}^<(-t_2))(iG_{2\gamma+1}^>(t_{34})) \{\Pi_{1+\gamma}^{<>} - \Pi_{1+\gamma}^{<<} + \Pi_{\gamma'}^{<>} - \Pi_{\gamma'}^{<<} + 2\Pi_{\gamma'}^{<>} - 2\Pi_{\gamma'}^{<<}\}. \quad (8)$$

Here, $\gamma = K_-^2 K$, $\gamma' = (K_-^2 + K_-)K$, and $t_{ij} = t_i - t_j$. The ordering on the Keldysh contour for a related problem is described in [21]. The factors of correlation functions,

$$iG_\beta^<(t) = \pm \frac{1}{2\pi\alpha} \frac{(\pi T \alpha / u)^\beta}{[\sin \pi T(\alpha / u \pm it)]^\beta}, \quad (9)$$

can be interpreted as the tunneling in and out density of states, and the Π -matrices,

$$\Pi_\beta^{\rho\sigma} = \frac{G_\beta^\rho(t_{23})G_\beta^\sigma(-t_4)}{G_\beta^\rho(-t_3)G_\beta^\sigma(t_{24})}, \quad (10)$$

describe the propagation of electrons along the wire. In principle, the current in equation (7) contains another term proportional to only $|\eta_2|^2$ that describes the tunneling of electrons into the probe from thermal excitations in the wire. However, for low temperatures ($T \ll E_1, E_2$), this contribution is exponentially suppressed.

The current for the chiral LL Eq. (2) can be derived in a similar fashion. First, we note that the Hamiltonian is analogous to that in Eq. (5), but with only one boson field, say ϕ_R , and with K replaced by the filling fraction ν . The tunneling Hamiltonian is identical to equation (6), and the electron operator is now bosonized as $\psi(x) = e^{i\phi_R(x)/\nu} / \sqrt{2\pi\alpha}$. The formal expression for the current is still given by equation (7). Using similar steps as above, one finds

$$I = e_0 |\eta_1|^2 |\eta_2|^2 \int_{-\infty}^{\infty} dt_2 dt_3 dt_4 e^{-iE_2 t_2 + iE_1 t_3} \times (iG_{1/\nu}^<(-t_2))(iG_{1/\nu}^>(t_{34})) \{\Pi_{1/\nu}^{<>} - \Pi_{1/\nu}^{<<}\}. \quad (11)$$

The correlation functions and the Π -matrices are again given by equations (9,10).

-
- [1] Mattis, D.C. and Lieb, E.H. Exact solution of a many fermion system and its associated boson field. *J. Math. Phys.* **6**, 304-312 (1965).
[2] Giamarchi, T. *Quantum Physics In One Dimension*. (Oxford University Press, Oxford, 2003).

-
- [3] Wen, X.G. Chiral Luttinger liquid and the edge excitations in the fractional quantum Hall states. *Phys. Rev. B* **41**, 12838-12844 (1990).
[4] Wen, X.G. Electrodynamical properties of gapless edge excitations in the fractional quantum Hall states. *Phys. Rev. Lett.* **64**, 2206 - 2209 (1990).
[5] Kane, C.L. and Fisher, M.P.A. Transmission through barriers and resonant tunneling in an interacting one-dimensional electron gas. *Phys. Rev. B* **46**, 15233-15262 (1992).
[6] Lorenz, T. *et al.* Evidence of spin-charge separation in quasi-one-dimensional organic conductors. *Nature* **418**, 614-617 (2002).
[7] Auslaender, O.M. *et al.* Spin-charge separation and localization in one dimension. *Science* **308**, 88-92 (2005).
[8] Le Hur, K., Halperin, B.I., and Yacoby, A. Charge fractionalization in nonchiral Luttinger systems. *Annals of Physics* **323**, 3037-3058 (2008).
[9] Steinberg, H. *et al.* Charge fractionalization in quantum wires. *Nature Physics* **4**, 116-119 (2008).
[10] Bockrath, M. *et al.* Luttinger-liquid behavior in carbon nanotubes. *Nature* **397**, 598-601 (1999).
[11] Yao, Z., Postma, H.W. Ch., Balents, L. and Dekker, C. Carbon nanotube intramolecular junctions. *Nature* **402**, 273-276 (1999).
[12] Milliken, F.P., Umbach, C.P. and Webb, R.A. Indications of a Luttinger liquid in the fractional quantum Hall regime. *Solid State Comm.* **97**, 309-313 (1996).
[13] Chang, A.M., Pfeiffer, L.N. and West, K.W. Observation of chiral Luttinger behavior in electron tunneling into fractional quantum Hall edges. *Phys. Rev. Lett.* **77**, 2538-2541 (1996).
[14] Grayson, M., Tsui, D.C., Pfeiffer, L.N., West, K.W. and Chang, A.M. Resonant tunneling into a biased fractional quantum Hall edge. *Phys. Rev. Lett.* **86**, 2645-2648 (2001).
[15] Chen, Y.-F., Dirks, T., Al-Zoubi, G., Birge, N.O. and Mason, N. Nonequilibrium tunneling spectroscopy in carbon nanotubes. *Phys. Rev. Lett.* **102**, 036804 (2009).
[16] Gutman, D.B., Gefen, Y. and Mirlin, A.D. Tunneling spectroscopy of Luttinger liquid structures far from equilibrium. *Phys. Rev. B* **80**, 045106 (2009).
[17] Bagrets, D.A., Gornyi, I.V. and Polyakov, D.G. Nonequilibrium kinetics of a disordered Luttinger liquid. Preprint at <http://arxiv.org/abs/0809.3166> (2008).
[18] Khodas, M., Pustilnik, M., Kamenev, A. and Glazman, L.I. Fermi-Luttinger liquid: Spectral function of interacting one-dimensional fermions. *Phys. Rev. B* **76**, 155402 (2007).
[19] Rammer, J. and Smith, H. Quantum field-theoretical methods in transport theory of metals. *Rev. Mod. Phys.* **58**, 323-359 (1986).

- [20] Chamon, C. de C. and Wen, X.G. Resonant Tunneling in the Fractional Quantum Hall Regime. *Phys. Rev. Lett.* **70**, 2605 - 2608 (1993).
- [21] Kane, C.L. and Fisher, M.P.A. Shot noise and the transmission of dilute Laughlin quasiparticles. *Phys. Rev. B* **67**, 045307 (2003).